Pressure-driven amplification and penetration of resonant magnetic perturbations

J. Loizu[1,2], S. R. Hudson[2], P. Helander[1], S. A. Lazerson[2], and A. Bhattacharjee[2]
[1] *Max-Planck-Institut für Plasmaphysik, D-17491 Greifswald, Germany*
[2] *Princeton Plasma Physics Laboratory, PO Box 451, Princeton NJ 08543, USA*
(Dated: November 29, 2016)

We show that a resonant magnetic perturbation applied to the boundary of an ideal plasma screw-pinch equilibrium with nested surfaces can penetrate inside the resonant surface and into the core. The response is significantly amplified with increasing plasma pressure. We present a rigorous verification of nonlinear equilibrium codes against linear theory, showing excellent agreement.

PACS numbers: 52.35.Ra, 52.35.Kt, 52.65.Ff

I. INTRODUCTION

Ideal magnetohydrodynamics (MHD) is routinely used to study highly conductive, magnetically confined plasmas [1]. However, fundamental difficulties in 3D ideal MHD arise from the existence of pressure-driven infinite currents around resonant rational surfaces [2, 3]. Historically this led to the conclusion that pressure must be fractal [2] or stepped [4]. Recently a new class of 3D ideal-MHD equilibria with nested surfaces has been proposed which allows for smooth pressure [5]. This class of equilibria exhibits current sheets at resonant surfaces that produce a jump in rotational transform. For this class of equilibria, all current densities are integrable and nested surfaces are preserved for arbitrary three-dimensional geometry. In particular, nonlinear 3D ideal-MHD equilibrium codes can be verified for the first time.

In this paper we consider, within this new theoretical framework, the linear and nonlinear ideal plasma response to a resonant magnetic perturbation (RMP) in a screw-pinch. We investigate the details of the structure of the current sheets and that of the pressure-driven Pfirsch-Schlüter current. We show that the RMP is amplified to large values as β is increased and that the perturbation penetrates inside the resonant surface. We perform an exact verification of nonlinear MHD codes against solutions to Newcomb equation. To our knowledge, these are the first equilibria with nested surfaces and smooth, finite pressure gradient across a resonant surface ever computed. Implications for experiments are discussed, in particular regarding equilibria where island-healing mechanisms are at play.

II. IDEAL RESPONSE TO AN RMP AT $\beta = 0$

In this section, we review and extend recent results on the calculation of the linear, ideal plasma response to an RMP in a screw pinch with zero pressure and no flow [5]. We show that the existence of flux-surfaces in the perturbed equilibrium is ensured by the presence of an axisymmetric current sheet on the resonant surface, which corresponds to a discontinuity in the rotational transform. A non-axisymmetric current sheet is also established as a necessary mechanism for a complete island shielding. The spatial structure of these currents is presented in detail. This section prepares the background necessary for Sec. III, where we provide novel predictions for the penetration and amplification of an RMP in finite-β equilibria.

A. Equilibrium

The axisymmetric, ideal-MHD equilibrium in a screw pinch with zero pressure and no flow satisfies

$$\frac{d}{dr}\Big[B_z^2(1+\iota^2\frac{r^2}{R^2})\Big]+\frac{2r\iota^2B_z^2}{R^2}=0\ , \tag{1}$$

where B_z is the axial field, $\iota = RB_\theta/rB_z$ is the rotational transform, B_θ is the poloidal field, and $2\pi R$ is the length of the cylinder. The equilibrium is fully determined by the value of the axial field at the origin, $B_z(0)$, the rotational-transform profile, $\iota(r)$, and the major and minor radius, R and a. We choose

$$\iota(r)=\begin{cases}\iota_0-\iota_1(r/a)^2+\Delta\iota/2 & \text{for} \quad r\le r_s\\ \iota_0-\iota_1(r/a)^2-\Delta\iota/2 & \text{for} \quad r\ge r_s\end{cases}$$

with ι_0 and ι_1 such that $\iota(r)$ jumps across the rational $\iota_s = 1/2$ at $r_s = a/2$, namely, $\iota(r_s) = \iota_s \pm \Delta\iota/2$. The solution for $B_z(r)$ can be obtained by integrating Eq. (1) from $r = 0$ to $r = r_s$, and then from $r = r_s$ to $r = a$, after imposing pressure continuity, $[[B^2]] = 0$, across the resonant surface. Here B is the total field and $[[\cdot]]$ is the jump across the surface. As a matter of fact, a finite jump in transform, $\Delta\iota > 0$, translates into a jump in both the poloidal and axial fields, $[[B_\theta]] \neq 0$ and $[[B_z]] \neq 0$. By virtue of Ampère's law, this implies the presence of an axisymmetric current sheet on the resonant surface (from now on denoted as DC current sheet). A discussion on the structure of this current is provided in Sec. II C. For $\Delta\iota = 0$, there is no such current and all equilibrium quantities are continuous and smooth. In that case, however, the equilibrium is not an analytical function of the boundary, namely, a perturbed equilibrium due to an arbitrarily small RMP and with persistent nested surfaces does not exist, as we shall now see.

B. Linear response to an RMP

The linear plasma displacement,

$$\boldsymbol{\xi} = \xi^r \mathbf{e}_r + \xi^\theta \mathbf{e}_\theta + \xi^z \mathbf{e}_z \ , \tag{2}$$

induced by a non-axisymmetric, radial perturbation with a single Fourier harmonic,

$$\xi^r(r=a,\theta,z) = \xi_a \cos(m\theta + kz) \ , \tag{3}$$

to the boundary satisfies the linearized force-balance equation,

$$\delta\mathbf{j}[\boldsymbol{\xi}] \times \mathbf{B}_0 + \mathbf{j} \times \delta\mathbf{B}[\boldsymbol{\xi}] = 0 \ , \tag{4}$$

where $\mathbf{B}_0$ is the equilibrium magnetic field and the linear, 'ideal' perturbation to the magnetic field is $\delta\mathbf{B}[\boldsymbol{\xi}] \equiv \nabla \times (\boldsymbol{\xi} \times \mathbf{B}_0)$, and $\delta\mathbf{j}[\boldsymbol{\xi}] \equiv \nabla \times \delta\mathbf{B}[\boldsymbol{\xi}]$. This reduces to Newcomb's equation [6],

$$\frac{d}{dr}\left(f\frac{d\xi}{dr}\right) - g\xi = 0, \tag{5}$$

where $\xi^r \equiv \xi(r)\cos(m\theta + kz)$. The functions $f(r)$ and $g(r)$ are determined by the equilibrium,

$$f = B_z^2(\iota - \iota_s)^2 \bar{k} r^2 \ , \tag{6}$$

$$g = \frac{f}{r^2}(k^2r^2 + m^2 - 1) + B_z^2(\iota_s^2 - \iota^2)2\bar{k}^2\iota_s^2 r \ , \tag{7}$$

where $k = -n/R$, $\iota_s = n/m$, and $\bar{k} = r/(R^2 + r^2\iota_s^2)$.

Figure 1 shows the result of numerical integration of Eq. (5) for an $m = 2$, $n = 1$ perturbation and for different values of $\Delta\iota$. The linear radial displacement is continuous and smooth provided $\Delta\iota > 0$, i.e. provided that there is a DC current sheet. However, for a continuous $\iota(r)$ that contains the resonance, $\iota = \iota_s$, Newcomb's equation is singular and the solution that is regular at the origin is $\xi(r < r_s) = 0$ and $\xi(r \geq r_s) \neq 0$, i.e. the radial displacement is discontinuous. This class of solutions is obtained by the linearly-perturbed, ideal equilibrium codes that are used to study non-axisymmetric boundary perturbations in tokamaks [7–9] and stellarators [10].

A discontinuous plasma displacement is inconsistent with the assumption of nested flux-surfaces: in fact, magnetic surfaces overlap if the displacement anywhere has $|d\xi/dr| > 1$. As can be inferred from Fig. 1, there must be a critical value for the magnitude of the DC current sheet above which $|d\xi/dr| < 1$ and thus for which the solution is consistent. An expression for the gradient of the displacement at the resonant surface was estimated analytically in Ref. [5],

$$|\xi_s'| = 2\iota_s' \frac{\xi_s}{\Delta\iota} \tag{8}$$

where $\xi_s \equiv \xi(r_s)$ and ι_s' is the shear around the resonant surface. Equation (8) can be obtained by studying the asymptotics of Eq. (5) for small values of $x = |(\iota - \iota_s)/\iota_s'|$.

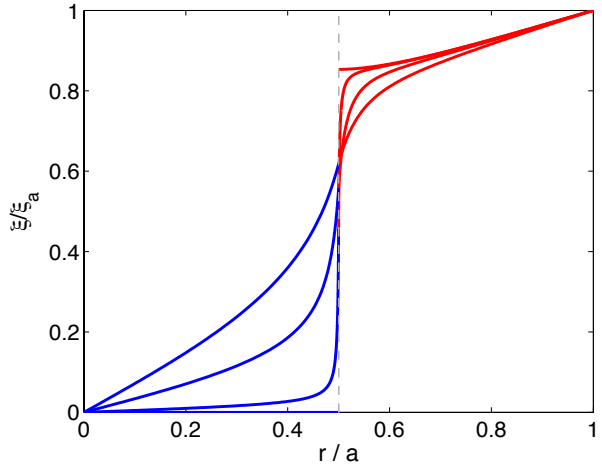

FIG. 1: Solutions of Eq. (5) for an $m = 2$, $n = 1$ boundary perturbation and for $\Delta\iota = 4 \times 10^{-2}, 10^{-2}, 10^{-3}$, and the singular case $\Delta\iota = 0$ (discontinuous curve). Colours merely indicate the inner ($r < r_s$, blue) and outer ($r > r_s$, red) parts of the solution.

Since ξ_s scales with ξ_a, we see that ξ_s' is proportional to the boundary perturbation and inversely proportional to $\Delta\iota$. The *sine qua non* condition for the existence of equilibria is $|\xi'| \leq 1$, which translates into $\Delta\iota \geq \Delta\iota_{min}$, where

$$\Delta\iota_{min} = 2\iota_s'\xi_s \ . \tag{9}$$

The continuous transform limit becomes a consistent solution as $\Delta\iota_{min} \to 0$, i.e. for infinitesimally small perturbation or infinitesimally small shear.

This analysis is linear and *a priori* limited to small boundary perturbations, $\xi_a/a \ll 1$; however, the prediction remains valid for the nonlinear calculations, as shown in Ref. [5].

We would like to note that even for a small, local change in the transform profile, i.e. a small jump $\Delta\iota$, the global solution is significantly different and the displacement penetrates inside the resonant surface all the way to the origin.

C. Structure of the current sheets

In general, a current sheet is present on a given flux surface if there exists a magnetic field discontinuity across this surface, $[[\mathbf{B}]] \equiv \mathbf{B}^+ - \mathbf{B}^- \neq 0$. In fact, by virtue of Ampère's law, $\mathbf{j} = \nabla \times \mathbf{B}$, this current sheet is given by

$$\mathbf{j} = [[\mathbf{B}]] \times \hat{\mathbf{n}}\ \delta(\mathbf{x} - \mathbf{x}_s) \tag{10}$$

where $\hat{\mathbf{n}}$ is the unit vector normal to the surface and $\mathbf{x}_s$ parametrizes points on the surface. We remark that $\mathbf{j}$ is strictly speaking a current *density* and that any physically valid current density must be integrable, so that the total current is finite. This is the case of Eq. (10).

In the system under consideration, namely a perturbed screw-pinch equilibrium, a discontinuity is present in the equilibrium field, $\mathbf{B}_0$, and in the perturbed field, $\delta\mathbf{B}$. The former gives rise to an axisymmetric or DC current sheet, while the latter produces a non-axisymmetric current sheet with a helicity corresponding to the resonant mode numbers. The fact that $[[\mathbf{B}_0]] \neq 0$ is a consequence of the discontinuous rotational transform defining the equilibrium. The reason for $[[\delta\mathbf{B}]] \neq 0$ is less obvious. The general expressions for the three components of the linearly perturbed field, $\delta\mathbf{B} = \nabla\times(\boldsymbol{\xi}\times\mathbf{B}_0)$, as a function of the radial displacement, $\xi_r = \xi(r)\exp[i(m\theta + kz)]$, are

$$\delta B_r = \frac{im}{R}B_z(\iota - \iota_s)\xi_r \tag{11}$$

$$\delta B_\theta = -h_1(r)\xi_r - \frac{m^2}{k^2r^2+m^2}\frac{r}{R}B_z(\iota-\iota_s)\xi_r' \tag{12}$$

$$\delta B_z = -h_2(r)\xi_r - \frac{krm}{k^2r^2+m^2}\frac{r}{R}B_z(\iota-\iota_s)\xi_r' \tag{13}$$

where

$$h_1(r) = B_\theta' + \frac{k}{k^2r^2+m^2}(krB_\theta + mB_z) \tag{14}$$

$$h_2(r) = B_z' + \frac{B_z}{r} - \frac{m/r}{k^2r^2+m^2}(krB_\theta + mB_z) \tag{15}$$

are defined by the equilibrium. In the particular case of continuous transform, the solution for ξ is discontinuous at $\iota = \iota_s$, thus it follows that $[[\delta\mathbf{B}]] \neq 0$ from Eqs. (12) and (13). In the case of discontinuous transform, the displacement ξ is continuous and smooth, but there still is a jump in $\delta\mathbf{B}$ because the products $(\iota-\iota_s)\xi_r$ and $(\iota-\iota_s)\xi_r'$ are discontinuous. This shows the general existence of a non-axisymmetric current sheet.

An important question is whether these current sheets are field-aligned, and if they are, whether they are aligned with the field on the inside or on the outside of the surface. We first consider the DC current sheet, which is given by

$$\mathbf{j}_{DC} = [[B_z]]\delta(r-r_s)\hat{\boldsymbol{\theta}} - [[B_\theta]]\delta(r-r_s)\hat{\mathbf{z}}\ . \tag{16}$$

The force produced by this current sheet and the equilibrium magnetic field is

$$\mathbf{j}_{DC}\times\mathbf{B}_0^{\pm} = ([[B_\theta]]B_\theta^{\pm} + [[B_z]]B_z^{\pm})\delta(r-r_s)\hat{\mathbf{r}} \tag{17}$$

where $\pm$ indicates either side of the surface. This force is non-zero in general, which would seem to contradict the fact that this is a force-free equilibrium. However, the sum of the two forces vanishes,

$$\mathbf{j}_{DC}\times\mathbf{B}_0^{+} + \mathbf{j}_{DC}\times\mathbf{B}_0^{-} = [[\mathbf{B}_0^2]]\delta(r-r_s)\hat{\mathbf{r}} = 0 \tag{18}$$

since the equilibrium satisfies $[[\mathbf{B}_0^2]] = 0$ by construction. This means that the current sheet is not aligned with either of the fields on each side of the surface, but rather aligned with the average surface field.

In general, the average $\mathbf{j}\times\mathbf{B}$ force produced by the *total* current sheet and the *total* magnetic field is also zero. Using $\mathbf{j} = [[\mathbf{B}]]\times\hat{\mathbf{n}}\delta(r-r_s)$, we have that

$$\mathbf{j}\times(\mathbf{B}^+ + \mathbf{B}^-) = [[\mathbf{B}^2]]\hat{\mathbf{n}} - (\mathbf{B}^+ + \mathbf{B}^-)\cdot\hat{\mathbf{n}}[[\mathbf{B}]] = 0 \tag{19}$$

since both $[[\mathbf{B}^2]] = 0$ and $\mathbf{B}\cdot\hat{\mathbf{n}} = 0$ are satisfied. Therefore, the current sheets are aligned such that the forces acting on each side of the surface are equal and opposite.

III. IDEAL RESPONSE TO AN RMP AT $\beta > 0$

We now consider the ideal response to an RMP in a screw-pinch with finite pressure and no flow. We show that even at modest values of β the perturbation can be significantly amplified and, as a consequence, penetrate inside the resonant surface with values exceeding the boundary perturbation amplitude. The results are confirmed by linear and nonlinear calculations.

A. Equilibrium

The axisymmetric, ideal-MHD equilibrium in a screw pinch with finite pressure and no flow satisfies

$$\frac{dp}{dr} + \frac{1}{2}\frac{d}{dr}\Big[B_z^2(1+\iota^2\frac{r^2}{R^2})\Big] + \frac{r\iota^2B_z^2}{R^2} = 0\ , \tag{20}$$

and is uniquely determined by the value of the axial field at the origin, $B_z(0)$, the rotational-transform profile, $\iota(r)$, the pressure profile, $p(r)$, and the major and minor radius, R and a. We choose

$$\iota(r) = \iota_0 - \iota_1(r/a)^2 \pm \Delta\iota/2\ ,$$
$$p(r) = p_0[1-2(r/a)^2 + (r/a)^4]\ ,$$

thus a continuous and smooth pressure profile such that $p(0) = p_0$ and $p(a) = 0$. The solution for $B_z(r)$ can be obtained by integrating Eq. (20) and imposing the continuity of the total pressure, $p + B^2/2$, across the resonant surface. Since p is continuous, this condition is $[[B^2]] = 0$.

We define β as computed at the origin,

$$\beta = \frac{2p(0)}{B_z^2(0)} \tag{21}$$

and variations in β will correspond to variations in $p(0)$.

B. Linear response to an RMP

The linearized force-balance equation still reduces to Newcomb's equation, Eq. (5), with the functions $f(r)$ and $g(r)$ given by

$$f = f|_{\beta=0}\ , \tag{22}$$

$$g = g|_{\beta=0} + \bar{k}\iota_s^2r^3p'\ , \tag{23}$$

where $f|_{\beta=0}$ and $g|_{\beta=0}$ are given by Eqs.(6) and (7), respectively. Thus the effect of the pressure gradient appears only in the function $g(r)$. As we shall see, this new term fundamentally changes the behaviour of ξ around the resonance surface.

Figure 2 shows the result of numerical integration of Eq. (5) for an $m = 2$, $n = 1$ perturbation, for a given value of $\Delta\iota$ and for different values of β. The perturbation is significantly amplified around the resonant surface, even at modest values of β. For example, at $\beta = 1\%$ the perturbation is amplified by a factor of $\xi_s/\xi_a \simeq 3$ on the resonant surface and penetrates all the way into the core with values exceeding the boundary perturbation, $\xi/\xi_a > 1$, for a significant fraction of the inner plasma column $r < r_s$. We also observe that the peak of the amplified perturbation is always occurring very close to - but not exactly at - the resonant surface. In order to quantify the amplification and penetration of the RMP, we define two quantities,

$$A_{rmp} = \frac{\xi_s}{\xi_a} \ , \tag{24}$$

$$P_{rmp} = 1 - \frac{r_*}{r_s} \ , \tag{25}$$

where r_* is the radius at which $\xi(r_*)/\xi_s = 1/e$. The meaning of A_{rmp} is quite obvious. The value of P_{rmp} measures the percentage of inner plasma column ($r < r_s$) in which the perturbation is still larger than ξ_s/e. For example, at $\beta = 1\%$, we have $A_{rmp} \simeq 3$ and $P_{rmp} \simeq 40\%$. Figures 3 and 4 show the dependence of A_{rmp} and P_{rmp} on β. Notice that the maximum amplitude of A_{rmp} and P_{rmp} depends on the magnitude of the DC current sheet, or $\Delta\iota$, that is assumed in the initial equilibrium. The question of what sets the value of $\Delta\iota$ in a plasma is discussed in Sec. V.

An important question is whether the initial axisymmetric equilibrium is interchange stable; for otherwise the results are not meaningful. A necessary (but not sufficient) condition for interchange stability in a screw-pinch is given by the Suydam criterion [1],

$$D_S = -\left(\frac{2p'\iota^2}{rB_z^2\iota'^2}\right)_s < \frac{1}{4} \ , \tag{26}$$

and the corresponding stability limit is shown in Figs. 3 and 4. While the actual stability limit can be reached slightly before Eq. (26) is violated, as can be seen from the lack of data points in Figs. 3 and 4, both the amplification and penetration of the RMP are already significantly large before this limit is attained.

Analytical understanding of the behaviour of the displacement around the resonant surface can be obtained by studying the asymptotics of Newcomb's equation. Expanding Eqs. (22) and (23) we have that

$$f \sim c_1 x^2 \ , \tag{27}$$

$$g \sim c_2 + O(x) \ , \tag{28}$$

for small $x = |(\iota - \iota_s)/\iota'_s|$, and where

$$c_1 = \left(\bar{k}B_z^2\iota'^2r^2\right)_s \ , \tag{29}$$

$$c_2 = \left(2\bar{k}\iota^2rp'\right)_s \ . \tag{30}$$

Inserting the antsatz $\xi \sim x^\alpha$ into Newcomb's equation, we find a quadratic equation for α, with solutions

$$\alpha = -\frac{1}{2} \pm \sqrt{\frac{1}{4} - D_S} \tag{31}$$

where $D_S = -c_2/c_1$ is the Suydam parameter, Eq. (26). At $\beta = 0$ we have that $D_S = 0$ and thus, from Eq. (31), $\alpha \in \{0, -1\}$. This explains why in Fig. 1 the displacement has finite ξ_s even for continuous-transform: the solution $\xi \sim x^0$ does not diverge for $x \to 0$. However, at finite $\beta > 0$, we have that $0 > D_S > 1/4$ and thus $\xi \sim \lambda_1 x^{\alpha_1} + \lambda_2 x^{\alpha_2}$, with

$$-1 < \alpha_1 < -\frac{1}{2} < \alpha_2 < 0 \ , \tag{32}$$

which necessarily implies that the displacement diverges unless x is never zero, namely, if and only if $\Delta\iota \neq 0$. Moreover, in order for the perturbed equilibrium to be physical, the DC current sheet must be sufficiently large to ensure that the *sine qua non* condition, $|\xi'| \leq 1$, is satisfied. This shows how important is the existence of this DC current sheet.

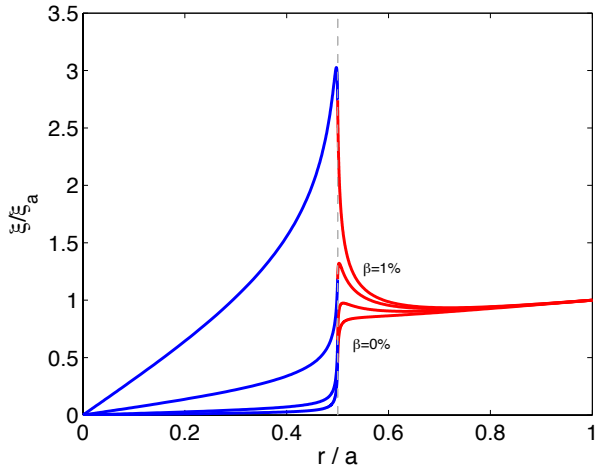

FIG. 2: Solutions of Eq. (5) for an $m = 2$, $n = 1$ boundary perturbation and for different values of β, from $\beta = 0\%$ (lower curve) to $\beta = 1\%$ (upper curve). For all cases $\Delta\iota = 10^{-3}$. Colours merely indicate the inner ($r < r_s$, blue) and outer ($r > r_s$, red) parts of the solution.

C. β-induced Pfirsch-Schlüter current

In addition to the current sheets established *on* the resonant surface, a pressure-driven Pfirsch-Schlüter current is expected to develop *around* the resonant surface.

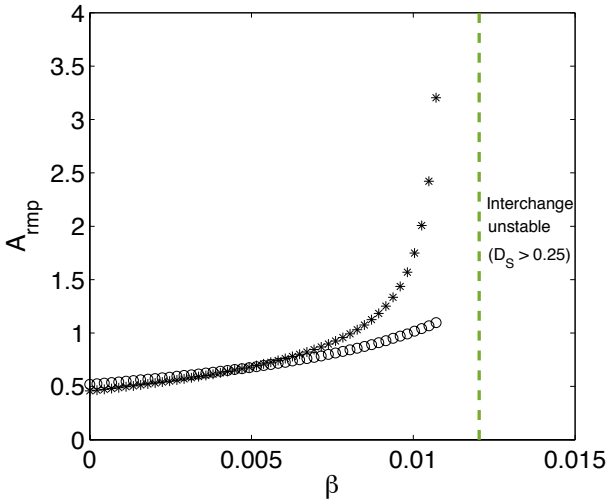

FIG. 3: Amplification of the RMP on the resonant surface as a function of β. Circles: $\Delta_t = 5\times10^{-3}$. Stars: $\Delta_t = 1\times10^{-3}$. The vertical dashed line indicates the critical β above which the Suydam criterion is not satisfied.

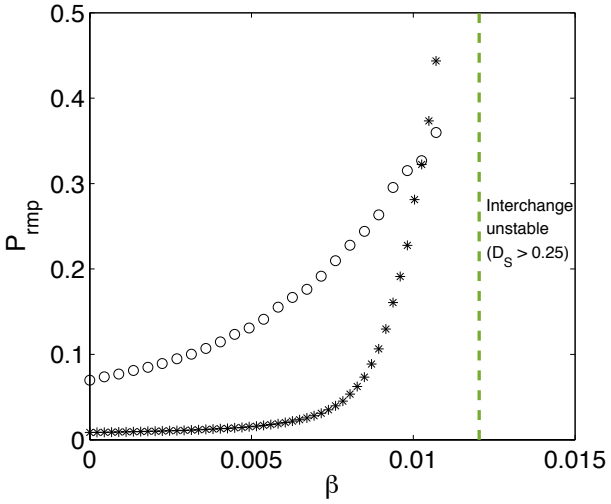

FIG. 4: Penetration of the RMP inside the resonant surface as a function of β. Circles: $\Delta_t = 5\times10^{-3}$. Stars: $\Delta_t = 1\times10^{-3}$. The vertical dashed line indicates the critical β above which the Suydam criterion is not satisfied.

Here we derive an analytical expression for the perturbed parallel current around the resonant surface in response to an RMP in a screw pinch. We show that the Pfirsch-Schlüter current can be large but is always integrable and bounded by $\xi p'/\Delta_t$.

For simplicity, we consider only the axial component of the perturbed current, δj_z, which corresponds to the perturbed parallel current, $\delta j_\parallel = (B_\theta \delta j_\theta + B_z \delta j_z)/B$, in the limit of a dominant axial field. The conclusions are the same in the general case where δj_θ is also considered.

The perturbed current, $\delta\mathbf{j} = \nabla\times(\nabla\times(\boldsymbol{\xi}\times\mathbf{B}_0))$, can be computed from the equilibrium field, $\mathbf{B}_0$, and the surface displacement, $\boldsymbol{\xi}$, which can be obtained from Newcomb's equation. One arrives to a general expression for δj_z of the form

$$\delta j_z = T_0(r)\xi + T_1(r)\xi' + T_2(r)\xi'' \tag{33}$$

where T_0, T_1, and T_2, are well-behaved functions. In particular, their behaviour around the resonant surface is $T_0(r) \sim T_1(r) \sim 1$ and $T_2(r) \sim O(x)$. The corresponding behaviour of the radial displacement and its derivatives is, for small β: $\xi \sim 1$, $\xi' \sim O(x^{-1})$, and $\xi'' \sim O(x^{-2})$. Thus it would seem that the current density around the resonant surface behaves as $1/x$, independently of pressure. However, it turns out that the large terms in Eq. (33), *i.e.* those that scale as $1/x$, balance each other by virtue of Newcomb's equation, Eq. (5), and the only large term left is

$$\delta j_z \sim \xi p'/x < \xi p'/\Delta_t \ . \tag{34}$$

Numerical evidence of this is shown in Fig. 5, where the profile of $\delta j_\parallel$ is computed from the solution of Newcomb's equation and by using Eq. (33). From the top panel in Fig. 5, one can see that the Pfirsch-Schlüter current is bounded even at $r = r_s$. The middle and bottom panels in Fig. 5 confirm the $1/x$-type behaviour at $\beta > 0$, exactly as predicted by Eq. (34).

To our knowledge, this is the first equilibrium with nested surfaces and smooth, finite pressure gradient across a resonant surface ever computed. As of now, however, these calculations are linear. We now show how nonlinear codes can also compute this class of equilibria and retrieve the linear results in the appropriate limit.

IV. VERIFCATION OF NONLINEAR CODES

Presently, the widely-used, three-dimensional, nonlinear ideal-MHD equilibrium codes VMEC [11] and NSTAB [12] are restricted to work with smooth functions and thus cannot handle discontinuities in the magnetic field (or current sheets). The SPEC code [13] does allow for discontinuities. SPEC formally finds extrema of the multi-region, relaxed, MHD (MRxMHD) energy functional, as proposed by Hole, Hudson and Dewar [14, 15]. In MRxMHD the magnetic topology is *discretely* constrained at a finite number, N, of so-called, "ideal" interfaces, where discontinuities in the pressure and tangential magnetic field are allowed. The volumes encapsulated by these ideal boundaries undergo Taylor relaxation, thus MRxMHD equilibria are not globally ideal; however, MRxMHD has been shown to exactly retrieve ideal MHD in the formal limit $N \to \infty$ [16], and SPEC was recently used to compute, for the first time, the singular current densities expected to form in three-dimensional ideal-MHD equilibria [17].

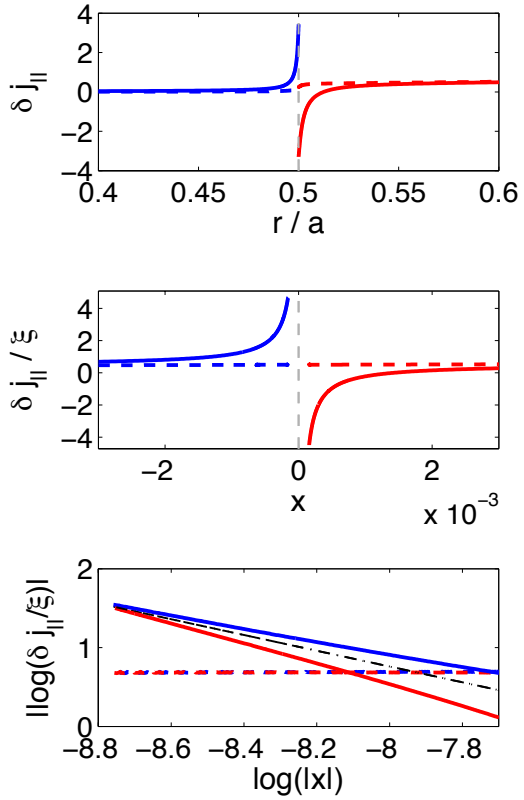

FIG. 5: Perturbed parallel current around the resonant surface, for $\beta = 0$ (dashed lines) and $\beta = 0.5\%$ (solid lines). Top: $\delta j_{||}$ as a function of the minor radius. Middle: $\delta j_{||}/\xi$ as a function of the distance x to the rational. Bottom: same as middle but in log-log scale. The dash-doted black line in the bottom panel has slope -1. Colours merely indicate the inner ($r < r_s$, blue) and outer ($r > r_s$, red) parts of the solution.

An exact verification of the SPEC code against solutions of Newcomb's equation, Eq. (5), was presented in a recent letter for the case of *zero-pressure* [5]. Here SPEC is employed to perform linear and nonlinear, ideal equilibrium calculations for the perturbed screw pinch with *finite* pressure. In the "ideal limit", i.e. very large N, the MRxMHD energy functional reduces to $W \equiv \int \left[p/(\gamma-1) + B^2/2\right] dv$. Equilibrium states are obtained when the gradient of this functional, $F[\mathbf{x}, b] \equiv \nabla p - \mathbf{j} \times \mathbf{B}$, is zero, where $\mathbf{x}$ represents the geometry of the internal flux-surfaces and where b denotes the dependence of the equilibrium on the prescribed boundary. Given an equilibrium state, i.e. $F[\mathbf{x}, b] = 0$, the first order correction to the internal geometry induced by a boundary deformation, δb, is defined by $\nabla_{\mathbf{x}} F \cdot \boldsymbol{\xi} + \nabla_b F \cdot \delta b = 0$, which is essentially Newcomb's equation generalized to arbitrary geometry, and the solution is $\boldsymbol{\xi} = -(\nabla_{\mathbf{x}} F)^{-1} \cdot \nabla_b F \cdot \delta b$. Figure 6 shows a comparison of the SPEC linear solutions and the corresponding Newcomb solutions, for different values of β. Each cross in Fig.6 corresponds to the radial displacement of each ideal interface considered in SPEC. The agreement between linear SPEC and linear theory is excellent.

Generally, nonlinear solutions to $F[\mathbf{x}, b] = 0$ for a given boundary are found by iterating on the linear correction, i.e. $\mathbf{x}_{i+1} \equiv \mathbf{x}_i - (\nabla_{\mathbf{x}} F)^{-1} \cdot F$, where i labels iterations. We perform a convergence study of the nonlinear SPEC equilibria towards the corresponding linear prediction as the boundary perturbation ξ_a is decreased. Excellent convergence is shown in Figure 7, with the error scaling as $e \sim O(\xi_a^2)$. The agreement arising from this verification exercise is of unprecedented nature and may shed some light on how to reconcile the recently observed discrepancies between linear and nonlinear equilibrium codes that assume nested flux surfaces [18, 19].

A verification of the VMEC code against the same linear theory has also been carried out recently in the case of *zero-pressure* [20]. VMEC cannot strictly compute equilibria with discontinuous rotational-transform; however nested flux surfaces are enforced by the representation of the magnetic field, and thus the solution that is obtained for the radial displacement, $\xi(r)$, is continuous and smooth, and always satisfies $|\xi'| \leq 1$. In fact, the VMEC solutions show a similar behaviour to that in Fig. 1 for the case of zero-pressure, when either the radial resolution or the shear are increased [20]. Figure 8 shows how VMEC calculations can reproduce a similar behaviour to that in Fig. 6 for the case of *finite* pressure. In particular, the phenomena of amplification and penetration of the boundary perturbation are observed as β is increased. In any case, while VMEC seems to qualitatively reproduce the ideal response to an RMP, an exact agreement with Newcomb's solutions may require explicit handling of discontinuities in the magnetic field.

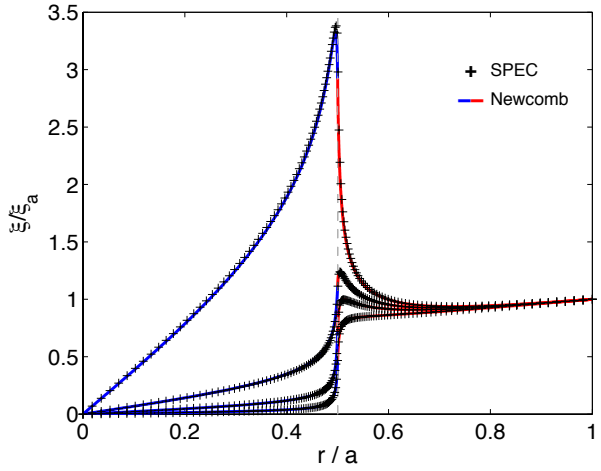

FIG. 6: SPEC linear solutions (crosses) and Newcomb solutions (solid lines) for an $m = 2$, $n = 1$ boundary perturbation and for different values of β, from $\beta = 0$ (lower curve) to $\beta = 1.1\%$ (upper curve). Here $\Delta_t = 1.4 \times 10^{-3}$.

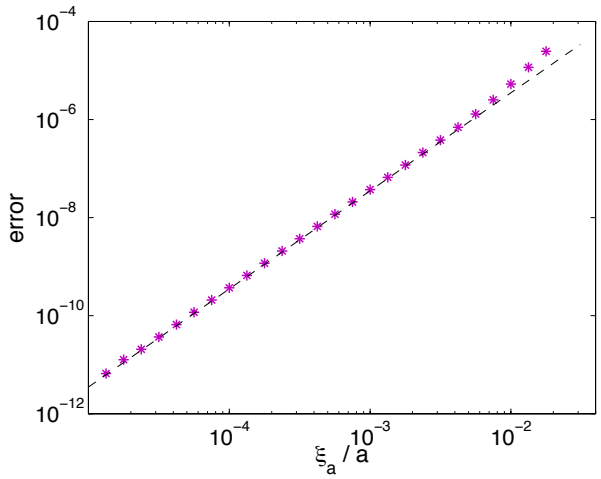

FIG. 7: Error between linear and nonlinear SPEC solutions for an $m = 2$, $n = 1$ boundary perturbation, $\beta = 0.1\%$, $\Delta\iota = 10^{-2}$, and for different values of the boundary perturbation amplitude ξ_a. Dashed line has slope 2.

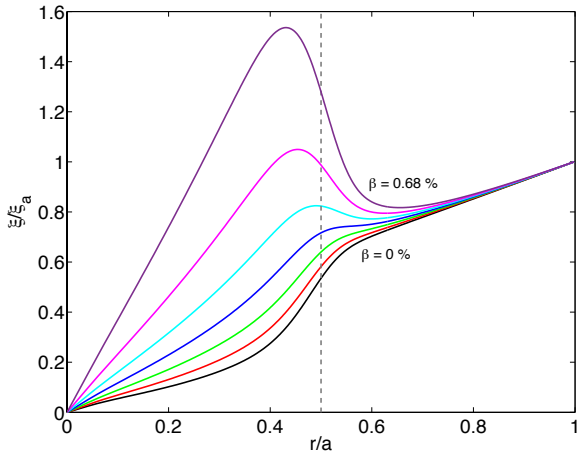

FIG. 8: VMEC perturbed equilibrium solutions for an $m = 2$, $n = 1$ boundary perturbation and for different values of β ranging from $\beta = 0$ (lower curve) to $\beta = 0.68\%$ (upper curve). Radial resolution corresponds to $N = 512$ flux-surfaces.

V. DISCUSSION AND CONCLUSIONS

We have shown that three-dimensional ideal-MHD equilibria with nested surfaces, arbitrarily smooth pressure gradient and discontinuous-transform across resonances are well defined and can be computed both linearly and nonlinearly. These states, we believe, may represent the only possible plasma equilibrium states with magnetic surfaces that are both nested *and* resonant.

Experimentally, it has been observed that under certain parameter regimes, magnetic islands forming around resonant surfaces in stellarators are healed [21]. Mechanisms responsible for self-healing of magnetic islands have been suggested [22, 23] and related to similar island dynamics observed in tokamaks [24]. However, regardless of *what mechanism is responsible for island-healing*, the resulting plasma equilibria should then be described by the class of equilibria considered herein. And our predictions seem to indicate that, in such a scenario, an RMP will be largely amplified around the resonance and will penetrate all the way into the core.

Two questions that remain to be answered are (1) what sets the value of $\Delta\iota$, and (2) how can these states be accessed?

Question (1) was partially answered in Ref. [5] by showing that there is a lower bound on the DC current sheet, $\Delta\iota > \Delta\iota_{min}$, which ensures that flux-surfaces are preserved. It remains to be investigated whether an upper bound exists. A close examination of the Rosenbluth solution [25] for the nonlinearly saturated ideal internal kink in a cylindrical tokamak, which is an example of three-dimensional ideal-MHD equilibrium with nested surfaces, is presented in Appendix A. The analysis shows that this equilibrium marginally satisfies the *sine qua non* condition, $|\xi'| \leq 1$, and thus this suggests that the current sheet on the resonant surface corresponds to $\Delta\iota = \Delta\iota_{min}$. However it may well be that other states with $\Delta\iota > \Delta\iota_{min}$ are also accessible, e.g. non-ideally. This will require further investigation.

Question (2) may be answered as follows. Assume that a plasma is initially in a perfectly axisymmetric state, i.e. with no resonances, and where the rotational-transform is continuous. Then the mechanism able to generate a jump in transform must obviously *not preserve* the functional $\iota(\Psi)$, where Ψ is a flux-surface label, e.g. the enclosed toroidal flux. Any non-ideal effect may provide such mechanism, although usually at the price of opening up an island; however, if the island is subsequently healed and a shielded state with nested surfaces is obtained, the final state may present a jump in the transform. Another much less intuitive mechanism was described by Eyink and Aluie [26], who showed that even within ideal-MHD, where the plasma is assumed to be infinitely conducting, the breaking of Alfvén's theorem is possible. In fact, the frozen-in-flux condition that is usually attributed to ideal plasmas results from combining Faraday's law and Ohm's law; however, in the presence of current and vorticity sheets, these two laws do not ensure the conservation of fluxes [26]. Such proof would suggest that a jump in transform could in principle be accessed even within ideal-MHD, although this also requires further investigation.

Acknowledgments

This work was carried out under the auspices of the Max-Planck-Princeton Center for Plasma Physics.

Appendix A: Current sheet in Rosenbluth's solution for the nonlinearly saturated ideal internal kink

The nonlinearly saturated ideal internal kink in a cylindrical tokamak was calculated by *Rosenbluth et al* [25] and is the classic example of three-dimensional ideal-MHD equilibrium with a resonant surface. This state results from an initially unstable axisymmetric equilibrium with a rational surface at $q = 1$. The final, ideally stable equilibrium has nested surfaces with an axisymmetric boundary, a current sheet on the resonant surface, and an inner helical plasma column with helicity $n = 1$, $m = 1$.

We now show that: (1) the solution for the displacement, ξ, of the flux-surfaces obtained by Rosenbluth marginally satisfies the *sine qua non* condition; (2) the conservation of toroidal flux is only ensured to zeroth order in ξ, thus making an equilibrium with a jump in ι of order $\Delta\iota \sim \xi$ consistent with Rosenbluth's solution; (3) the current sheet predicted on the resonant surface has a DC component and thus is consistent with the existence of a jump in transform.

The nonlinear solution for the displacement is given by Eq. (23) in Ref. [25],

$$\xi(x,\theta) = \int_0^x \Big[\frac{x'}{\sqrt{f(x')+g(\theta)}} - 1\Big]dx' + h(\theta) \qquad \text{(A1)}$$

where θ is the polar angle and ξ is the radial displacement of a flux surface originally situated at a radius x with respect to the resonant surface ($x = 0$ is the original radius of the resonant surface). The new radius of a flux surface starting at x is then, by definition,

$$r = x + \xi(x,\theta) \qquad \text{(A2)}$$

which is Eq.(22) in Ref. [25]. From Eq. (A1) we find the gradient of the displacement at the resonant surface,

$$\frac{\partial\xi}{\partial x}\Big|_{x=0} = -1 \ , \qquad \text{(A3)}$$

which marginally satisfies the *sine qua non* condition for the existence of equilibria, namely $|\xi'| \leq 1$.

The nonlinearly saturated state is found by evolving the plasma parameters under ideal constraints. Among these constraints is the conservation of toroidal flux, which is imposed in Eq.(19) of Ref. [25],

$$\int_{\tau_H} r dr d\theta = \int_{\tau_c} r dr d\theta \qquad \text{(A4)}$$

where the helical and cylindrical areas of integration, τ_H and τ_c, are defined for a given flux-surface. Equation (A4) represents the conservation of areas and thus corresponds to the conservation of toroidal flux in the limit of constant B_z. Then, in Ref.[25], Eq. (A4) is differentiated with respect to x, giving

$$\oint r\frac{\partial r}{\partial x}d\theta = \oint r_c\frac{\partial r_c}{\partial x}d\theta = x \qquad \text{(A5)}$$

where the last equality comes from the fact that $r_c = x$ by construction. Finally, combining Eqs. (A1) and (A2) into Eq. (A5), one gets

$$\oint (x+\xi)\frac{x}{\sqrt{f(x)+g(\theta)}}d\theta = x \ . \qquad \text{(A6)}$$

In Ref. [25], the term ξ in Eq. (A6) is neglected, leading to a fundamental relation,

$$\oint \Big[f(x)+g(\theta)\Big]^{-1/2}d\theta = x^{-1} \ , \qquad \text{(A7)}$$

which corresponds to Eq.(24) in Ref. [25]. However this relation is, as we have shown, only valid to zeroth order in ξ. Therefore, the conservation of toroidal flux is only enforced to zeroth order in ξ. In other words, any solution that violates flux conservation up to order ξ is still consistent with Rosenbluth's solution.

Finally, we briefly consider the structure of the current sheet in Rosenbluth's solution. As stated in Ref. [25], the integrated current sheet has magnitude

$$\int J dr = [g(\theta)]^{1/2}, \qquad \text{(A8)}$$

and since $g(\theta) \sim \xi^2 \cos^8(\theta/2)$ we have that

$$\int J dr \sim \xi \cos^4(\theta/2) \ . \qquad \text{(A9)}$$

According to Eq. (A9), the magnitude of the current sheet scales linearly with ξ, as in our theory [5]. Moreover, a Fourier decomposition of the function $\cos^4(\theta/2)$ reveals the presence of $m = 0$, $m = 1$, and $m = 2$ components in the expression for the current. Thus, there is a "DC" component ($m = 0$) in the current sheet, consistent with the existence of a jump in the rotational transform of order $\Delta\iota \sim \xi$.

[1] Jeffrey P. Freidberg. *Ideal MHD.* Cambridge University Press, 2014.

[2] H. Grad. Toroidal Containment of a Plasma. *Physics of Fluids*, 10(1):137, 1967.

[3] P. Helander. Theory of plasma confinement in non-axisymmetric magnetic fields. *Reports on Progress in Physics*, 77(8):087001, August 2014.

[4] Oscar P. Bruno and Peter Laurence. Existence of three-dimensional toroidal MHD equilibria with nonconstant pressure. *Communications on Pure and Applied Mathe-*

matics, 49(7):717–764, July 1996.

[5] J. Loizu, S. R. Hudson, a. Bhattacharjee, S. Lazerson, and P. Helander. Existence of three-dimensional ideal-magnetohydrodynamic equilibria with current sheets. *Physics of Plasmas*, 22(9):090704, September 2015.

[6] William A Newcomb. Hydromagnetic stability of a diffuse linear pinch. *Annals of Physics*, 10(2):232–267, June 1960.

[7] D H Liu and A Bondeson. Improved poloidal convergence of the MARS code for MHD stability analysis. *Computer Physics Communications*, 116(98), 1999.

[8] J. Park, A. H. Boozer, and A. H. Glasser. Computation of three-dimensional tokamak and spherical torus equilibria. *Physics of Plasmas*, 14(5):052110, 2007.

[9] N.M. Ferraro and S.C. Jardin. Calculations of two-fluid magnetohydrodynamic axisymmetric steady-states. *Journal of Computational Physics*, 228(20):7742–7770, November 2009.

[10] C. Nuhrenberg and A. H. Boozer. Magnetic islands and perturbed plasma equilibria. *Physics of Plasmas*, 10(7):2840, 2003.

[11] S. P. Hirshman. Steepest-descent moment method for three-dimensional magnetohydrodynamic equilibria. *Physics of Fluids*, 26(12):3553, 1983.

[12] Mark Taylor. A High Performance Spectral Code for Nonlinear MHD Stability. *Journal of Computational Physics*, 110(2):407–418, February 1994.

[13] S. R. Hudson, R. L. Dewar, G. Dennis, M. J. Hole, M. McGann, G. von Nessi, and S. Lazerson. Computation of multi-region relaxed magnetohydrodynamic equilibria. *Physics of Plasmas*, 19(11):112502, 2012.

[14] M.J Hole, S.R Hudson, and R.L Dewar. Equilibria and stability in partially relaxed plasmavacuum systems. *Nuclear Fusion*, 47(8):746–753, August 2007.

[15] S. R. Hudson, M. J. Hole, and R. L. Dewar. Eigenvalue problems for Beltrami fields arising in a three-dimensional toroidal magnetohydrodynamic equilibrium problem. *Physics of Plasmas*, 14(5):052505, 2007.

[16] G. R. Dennis, S. R. Hudson, R. L. Dewar, and M. J. Hole. The infinite interface limit of multiple-region relaxed magnetohydrodynamics. *Physics of Plasmas*, 20(3):032509, 2013.

[17] J. Loizu, S. Hudson, A. Bhattacharjee, and P. Helander. Magnetic islands and singular currents at rational surfaces in three-dimensional magnetohydrodynamic equilibria. *Physics of Plasmas*, 22(2):022501, February 2015.

[18] A. D. Turnbull, N. M. Ferraro, V. A. Izzo, E. A. Lazarus, J.-K. Park, W. A. Cooper, S. P. Hirshman, L. L. Lao, M. J. Lanctot, S. Lazerson, Y. Q. Liu, A. Reiman, and F. Turco. Comparisons of linear and nonlinear plasma response models for non-axisymmetric perturbations. *Physics of Plasmas*, 20(5):056114, 2013.

[19] A. Reiman, N.M. Ferraro, A. Turnbull, J.K. Park, A. Cerfon, T.E. Evans, M.J. Lanctot, E.a. Lazarus, Y. Liu, G. McFadden, D. Monticello, and Y. Suzuki. Tokamak plasma high field side response to an n = 3 magnetic perturbation: a comparison of 3D equilibrium solutions from seven different codes. *Nuclear Fusion*, 55(6):063026, June 2015.

[20] S Lazerson, J Loizu, S Hudson, and S. P. Hirshman. Verification of the ideal-MHD response at rational surfaces in VMEC. *Physics of Plasmas, submitted*, 2015.

[21] Y. Narushima, K.Y. Watanabe, S. Sakakibara, K. Narihara, I. Yamada, Y. Suzuki, S. Ohdachi, N. Ohyabu, H. Yamada, and Y. Nakamura. Dependence of spontaneous growth and suppression of the magnetic island on beta and collisionality in the LHD. *Nuclear Fusion*, 48(7):075010, July 2008.

[22] A. Bhattacharjee, T. Hayashi, C. C. Hegna, N. Nakajima, and T. Sato. Theory of pressure-induced islands and self-healing in three-dimensional toroidal magnetohydrodynamic equilibria. *Physics of Plasmas*, 2(3):883, 1995.

[23] C. C. Hegna. Plasma flow healing of magnetic islands in stellarators. *Physics of Plasmas*, 19(5):056101, 2012.

[24] S. M. Wolfe, I. H. Hutchinson, R. S. Granetz, J. Rice, a. Hubbard, a. Lynn, P. Phillips, T. C. Hender, D. F. Howell, R. J. La Haye, and J. T. Scoville. Nonaxisymmetric field effects on Alcator C-Mod. *Physics of Plasmas*, 12(5):056110, 2005.

[25] M. N. Rosenbluth, R. Y. Dagazian, and P. H. Rutherford. Nonlinear properties of the internal m = 1 kink instability in the cylindrical tokamak. *Physics of Fluids*, 16(11):1894, 1973.

[26] Gregory L. Eyink and Hussein Aluie. The breakdown of Alfvéns theorem in ideal plasma flows: Necessary conditions and physical conjectures. *Physica D: Nonlinear Phenomena*, 223(1):82–92, November 2006.